THE JOURNAL OF PHYSICAL CHEMISTRY C
A JOURNAL OF THE AMERICAN CHEMICAL SOCIETY

pubs.acs.org/JPCC

Article

Understanding the Electrokinetic Role of Ions on Electricity Generation in Droplet-Based Hydrovoltaic Systems

Min Sung Kang, Hyunseok Ko, Seokhee Lee,* and Sung Beom Cho*

Cite This: *J. Phys. Chem. C* 2023, 127, 16811−16817

Read Online

ACCESS | Metrics & More | Article Recommendations | Supporting Information

ABSTRACT: Hydrovoltaic is emerging as a promising energy harvesting technology with the remarkable capability of generating energy through the direct interaction of water and material. The hydrovoltaic generates volt-level potentials without any external force, and its electrical performance can be enhanced by using an aqueous solution. However, it is not clear how salt ions affect or interact with the material. Herein, the theoretical model was used to provide an in-depth analysis of working principles. The model, validated with experimental results, incorporates four physics: water flow in unsaturated porous media, transportation of ions, chemical reactions, and electrostatics. It was found that the distribution of ions is key to improving the voltage output. The higher gradient of ions' concentration leads to strong potential differences, and its asymmetry of concentration is mainly governed by the water flow and concentration distribution. Additionally, we analyzed the parametric effects of substrate porosity and relative humidity under salt solution. The results showed that the presence of salt ions makes the electrical performance highly sensitive to porosity but less sensitive to relative humidity. Our findings improve the understanding of hydrovoltaic mechanisms and pave the way for the practical use of hydrovoltaic systems.

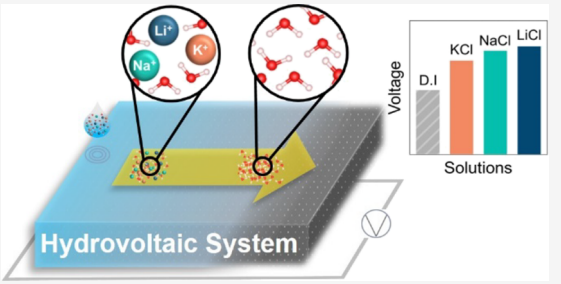

1. INTRODUCTION

Hydrovoltaic is an emerging technology in the field of energy harvesting due to the ubiquitous nature of water. Contrary to conventional hydroelectric technology, which generates energy indirectly through the kinetic energy of water, hydrovoltaic produces electricity through the direct interaction between water and a nanostructured material.[1,2] To improve the performance of electricity generation, numerous efforts are underway to explore the diverse materials such as carbons,[3,4] graphene oxides,[5,6] nanowires,[7−10] and polymers.[11,12] These advances have allowed hydrovoltaic technology to generate electricity at a voltage-order level of energy, enabling energy applications such as battery-less sensors[13,14] and power supplies.[15−17] Although hydrovoltaic technology holds promising potential, its current applications are still limited to laboratory-level demonstrations due to the lack of understanding of the mechanisms involved in electricity generation.[18] This lack of understanding creates a bottleneck for the optimization strategy of material and enhancing performance. Therefore, it is crucial to develop a deeper understanding of the electricity generation mechanisms to further advance hydrovoltaic systems.[19,20]

Since the introduction of hydrovoltaic technology, many studies have proposed hypotheses about the mechanisms of the electricity generation process, such as streaming potential,[21,22] ionovoltaic effect,[23] pseudo-streaming current,[4] and concentration gradient of charge carriers.[24] Based on these recent advances in the mechanistic studies, the principles of electricity generation in hydrovoltaic can be classified into two types:[19] water flow-induced (e.g., streaming potential,[21,22] electron drag,[25] and pseudo-streaming current[4]) and ion diffusion-induced (e.g., ionovoltaic effect[23] and the gradient of protons or ions[24]). However, there is still an ongoing debate about which mechanism dominantly influences the output. This is because identifying the exact mechanism is difficult due to the varying experimental conditions including humidity and substrate porosity in each experiment. In this regard, Ko *et al.*[26] recently conducted theoretical analyses to demonstrate which mechanism has the most dominant effect on the electric output of hydrovoltaic. It was revealed that the ion concentration gradient contributes more dominantly to electricity generation than the streaming potential under DI water conditions, and we also analyzed the parametric effect (e.g., porosity, substrate geometry, chemical reaction, etc.) to improve the output voltage.

Recently, numerous practical devices have been reported that operate under an aqueous solution, and it has been observed that the presence of salt affects the performance of electricity. Wu *et al.*[27] have reported that a water-evaporation-induced electricity generator produces around 2-fold open-

Received: May 14, 2023
Revised: August 8, 2023
Published: August 22, 2023

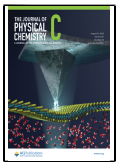

circuit voltage in NaCl solution compared to that in DI water. Additionally, Yun *et al.*[4] have conducted a series of voltage measurements on droplet-based hydrovoltaic systems in DI water and various salt solutions, and the results show that electrolytes generate significantly higher voltages compared to DI water. Although these previous studies suggested that the performance improvement is related to the electrical double layer (EDL), the exact working principle is still unclear because there are still phenomena that the conventional electrokinetic effect cannot explain. For example, Jin *et al.*[23] drop the NaCl solution with varying the concentration on the porous CuO nanowire film and found that the movement of ions (i.e., ionovoltaic effect) is the main driving force for the electrical output in hydrovoltaic. Therefore, it is necessary to investigate the mechanism of the salt effect on the electricity generation of hydrovoltaic applications for widespread use in practical real-world applications.

In this work, we investigated the voltage generation mechanism of salt ions in a droplet-based hydrovoltaic system using DI water and LiCl, NaCl, and KCl solutions by comparing the finite-element method (FEM) and experimental methods directly. We constructed the multiphysics model including fluid dynamics, diffusion dynamics, chemical reaction, and electrostatics to describe the ionic effects and related the hydrovoltaic effects on a droplet-based hydrovoltaic device. To analyze the effect of salt ions on voltage generation, we examined the ion concentrations of each species and the driving forces of salt ions with time. Our results show that the distribution of ion concentrations is the dominant factor in electricity generation. Interestingly, we found that the driving force of salt ions and protons is very different. The movement of salt ions is mainly governed by convection and diffusion, whereas the flow of protons is mainly influenced by diffusion and electrophoresis. We also conducted a parametric study by varying the porosity and evaporation rates to further understand the system's behavior. From these results, our work paves the way to achieve the practical use of hydrovoltaic systems.

2. METHODS

2.1. Experimental Section. For the fabrication of the hydrovoltaic device, carbon black (CB) inks were prepared by dispersing 0.5 g of carbon black powder (Alfa Aesar) in DI water (60 mL) with 0.2 g of a sodium dodecylbenzenesulfonate (SDBS, Sigma-Aldrich) surfactant. To achieve a uniform dispersion of CB inks, the solution was subjected to ball milling using balls of both 3 and 5 mm sizes. Then, cotton fabric (3 cm × 9 cm × 0.2 mm) was dipped into CB inks and dried in an oven at 80 °C for 30 min (the photograph of the carbon black-coated cotton fabric is shown in Figure S1). The measured resistance of CB-coated cotton fabric is 1 MΩ. The electrical performance (open-circuit voltage) was measured in real time using a ZIVE SP2 potentiostat (Wonatech). All experiments were conducted with 0.3 mL solutions under 60% of relative humidity (RH). To investigate the effect of salt, DI water and 0.1 M solutions of LiCl, NaCl, and KCl were used.

2.2. Theoretical Model of Hydrovoltaic. A hydrovoltaic device using a carbon-coated porous substrate with dimensions close to real devices was modeled using the finite-element method (FEM). This model includes four different types of physics: (i) flow in an unsaturated porous medium, (ii) chemical reaction, (iii) ion transport, and (iv) electrostatics. FEM was used to calculate the electrical properties using COMSOL Multiphysics software, which solves the coupled equations. The following four COMSOL modules were used: porous media and subsurface flow, chemistry, transport of diluted species, and electrostatics. Table 1 shows the values of the parameters used in this simulation model compared to the previous study. For more detailed parameter notations and values, refer to Tables 1 and 2 in the previous study.[26]

Table 1. Values of the Parameters Used in the Hydrovoltaic Model

symbol	description	value [unit]
D_{Cl^-}	diffusivity of Cl^- in water	1.97×10^{-9} [m^2/s]
D_{Li^+}	diffusivity of Li^+ in water	1.03×10^{-9} [m^2/s]
D_{LiCl}	diffusivity of LiCl in water	1.366×10^{-9} [m^2/s]
D_{Na^+}	diffusivity of Na^+ in water	1.333×10^{-9} [m^2/s]
D_{NaCl}	diffusivity of NaCl in water	1.61×10^{-9} [m^2/s]
D_{K^+}	diffusivity of K^+ in water	1.893×10^{-9} [m^2/s]
D_{KCl}	diffusivity of KCl in water	1.993×10^{-9} [m^2/s]
c_{LiCl}	initial concentration of LiCl	100 [mol/m^3]
c_{NaCl}	initial concentration of NaCl	100 [mol/m^3]
c_{KCl}	initial concentration of KCl	100 [mol/m^3]
ρ_{LiCl}	molar weight of LiCl	42.419 [g/mol]
ρ_{NaCl}	molar weight of NaCl	58.441 [g/mol]
ρ_{KCl}	molar weight of KCl	74.549 [g/mol]

Once a solution droplet falls on one side of the carbon black (CB) sheet (left side in the model), this was followed by solution spreading on and through the porous CB. To describe this movement of solution through porous media in the hydrovoltaic system, we introduced Richard's equation.[28] Richard's equation for the fluid flow u in a medium with a porosity of ϵ_p can be written as

$$\frac{\partial}{\partial t}(\epsilon_p \rho) + \nabla \cdot (\rho u) = Q_m \tag{1}$$

where Q_m is the mass source; it is equal to the pore change rate plus the change rate of the fluid flow. Additionally, evaporation is crucial in the hydrovoltaic system because it highly affects the flow of water. Evaporation strongly depends on the vapor pressure difference between the atmosphere (p_{VA}) and the water surface (p_{VS}). Therefore, the evaporation rate (E_v, kg·m^{-2} s^{-1}) is expressed as

$$E_v = -X_E \epsilon_p \rho \cdot (p_{VS} - p_{VA}) \tag{2}$$

where X_E is a scaling factor of dynamic evaporation resistance of the CB sheet (s·m^{-1}) that couples porosity to evaporation rate. This factor affects the amount of water remaining in the substrate, and its value is determined within a reasonable range by comparing it with the experimental voltage results.

We considered five possible chemical reactions in this model:

$$H_2O \leftrightarrow H_3O^+ + OH^- \tag{R1}$$

$$(C - OH) + H_2O \leftrightarrow (C - O)^- + H_3O^+ \tag{R2}$$

$$KCl \leftrightarrow K^+ + Cl^- \tag{R3}$$

$$LiCl \leftrightarrow Li^+ + Cl^- \tag{R4}$$

$$NaCl \leftrightarrow Na^+ + Cl^- \tag{R5}$$

where reaction R1 is the natural dissociation of water at pH = 7, reaction R2 is the protonation process where protons are

https://doi.org/10.1021/acs.jpcc.3c03183
J. Phys. Chem. C 2023, 127, 16811−16817

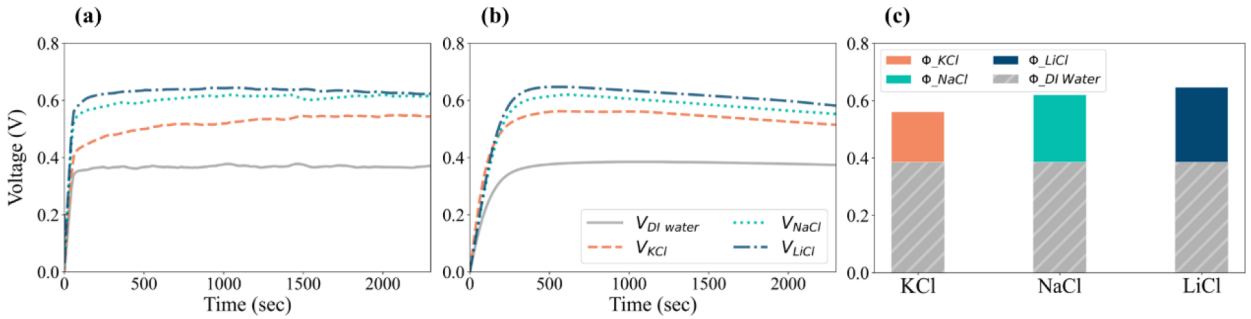

Figure 1. (a) Voltage profile of the experiment and (b) simulation model. The voltage was measured in 0.3 mL of DI water (gray), KCl (orange), NaCl (cyan), and LiCl (navy). (c) Maximum voltage generated by each solution and its proportion (Φ) of the effect on voltage generation compared to DI water in the simulation model.

transferred between water and functional groups on the substrate surface, and reactions R3−R5 are the natural dissociation of salts in water. In this study, we considered H_3O^+, OH^-, K^+, Na^+, and Li^+ as the mobile charge carriers, while $(C{-}O)^-$ is considered the functional group in our system due to the hydroxyl groups being the predominant groups on the surface of the carbon-coated cotton fabric, as shown in Figure S2. Then, these chemical species are transported to the right of the substrate by convection, diffusion, and electrokinetics. Because there is no species production and ionic drift in this study, the concentration of ionic species i (c_i) can be described by conservation of mass via the Nernst−Planck equation

$$\frac{\partial c_i}{\partial t} + \nabla \cdot J_i = 0 \tag{3}$$

where (J_i) is the ionic flux; it can also be expressed as

$$J_i = -\left[-uc_i + D_i \nabla c_i + \frac{D_i z_i F}{k_B T} c_i \nabla \phi\right] \tag{4}$$

where D_i is the diffusion coefficient of chemical species i, z_i is the valence charge of i, and ϕ is the electrostatic potential. The three terms on the right side of eq 4eq 4 represent the convective flux (coupled to fluid flow in a porous medium), the diffusive flux (Fick's law), and the electrophoretic flux (coupled to an electric field), respectively.

The electrostatic potential and electric field are coupled with the concentration distribution of ions. Therefore, the electrostatic potential and electric field can be calculated using the Poisson equation

$$\nabla^2 \phi = -\frac{\rho_V}{\varepsilon_0 \varepsilon_r} \tag{5}$$

where ε_0 is the vacuum permittivity (8.854×10^{-12} F/m), ε_r is the unitless relative permittivity, and ρ_V is the charge density. ρ_V can also be expressed as $\Sigma z_i e c_i$, where c_i is the concentration of ions. In this study, we assumed that the mobile ions were limited to H_3O^+, OH^-, K^+, Na^+, Li^+, and Cl^-. In addition, the streaming potential that arises from the development of an electric double layer on a wall due to fluid flow caused by pressure was solved by using the Helmholtz−Smoluchowski equation:[20]

$$V_{str} = \Delta P \cdot \frac{\varepsilon_0 \varepsilon_r \zeta}{\eta K_l} \tag{6}$$

where ΔP is the hydraulic pressure difference between the left and right side of the substrate, ζ is the zeta potential of the carbon material obtained from experimental measurements, η is the dynamic viscosity of the liquid, and K_l is the specific conductivity of the liquid.

The open-circuit voltage (V_{OC}) was measured by taking the surface potential difference between the two end regions of the substrate, while a relative humidity (RH) of 60%, a temperature of 20 °C, and ambient atmospheric pressure of 1 atm were set as the standard conditions.

3. RESULTS AND DISCUSSION

3.1. Hydrovoltaic Model Design. To investigate the effect of salt ions on droplet-based hydrovoltaic systems, we utilized an approach that combines both experimental and simulation methods. The experimental results were obtained by dropping 0.3 mL solutions, including DI water, LiCl, NaCl, and KCl, onto the negative electrode (left side) of a dry substrate coated with carbon black (CB), while jigs were connected on both sides to measure the voltage. We investigate the effect of the presence of salt on the voltage output and compare the impact of different salt ions by using various solutions. The measured voltage profiles for four different solutions are shown in Figure 1a. The results show that the voltage can be increased by salt ions, and LiCl, NaCl, and KCl produce the highest output in that order.

Based on the experimental model, the simulation model incorporates four physical phenomena: water flow in an unsaturated porous medium, chemical reactions, transport of dilute species, and electrostatics. In addition, the parameters' value of the simulation model was obtained through both first-principles calculations and previous literature to match the experimental conditions. More details are described in the Methods section. The voltage profiles for four different solutions: DI water, LiCl, NaCl, and KCl, were calculated using simulation models, as shown in Figure 1b. Although the simulation results took slightly longer to reach the maximum voltage than the experimental data (Figure 1a) due to differences in the jigs' connection area, the overall tendency of the voltage profile, including the rapid initial increase and gradual decrease, and the maximum value of the open-circuit voltage were consistent with our experimental results and previous study.[4] The voltage profiles clearly demonstrated that the addition of salt to the solution significantly enhanced voltage generation compared to pure DI water. To further quantify the effect of salt on voltage generation, we compared DI water to salt solutions in Figure 1c. Notably, LiCl showed

https://doi.org/10.1021/acs.jpcc.3c03183
J. Phys. Chem. C 2023, 127, 16811−16817

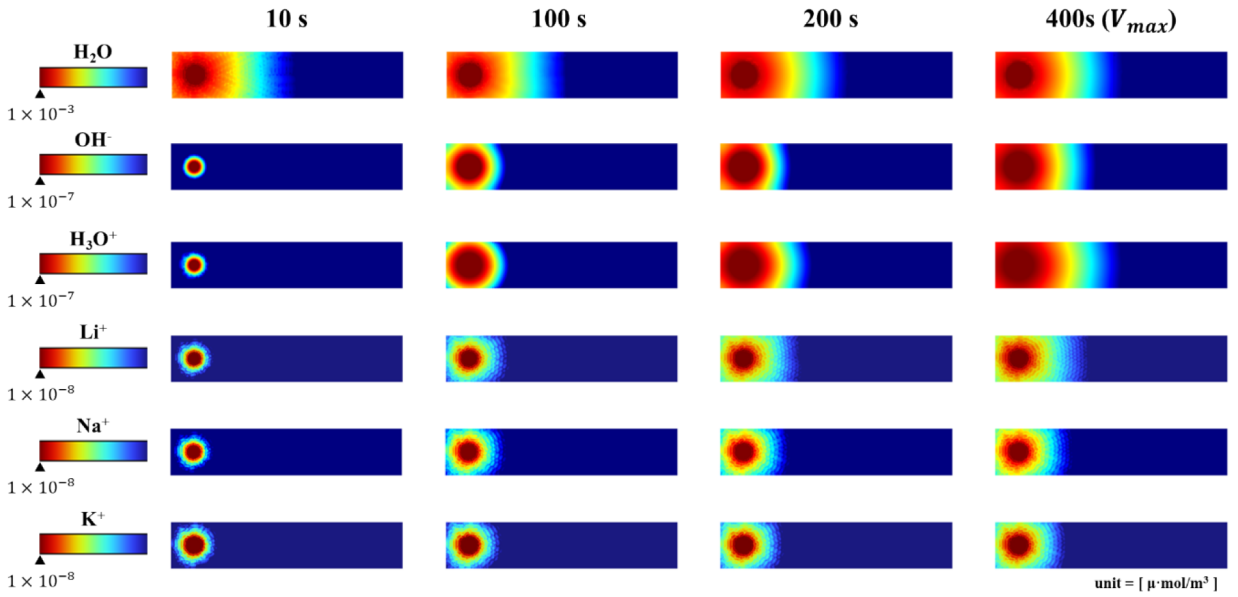

Figure 2. Surface concentrations of chemical species. The values on the scale bars represent the maximum concentration values throughout the simulation time. Note that the scales are adjusted to improve visibility at each timestep.

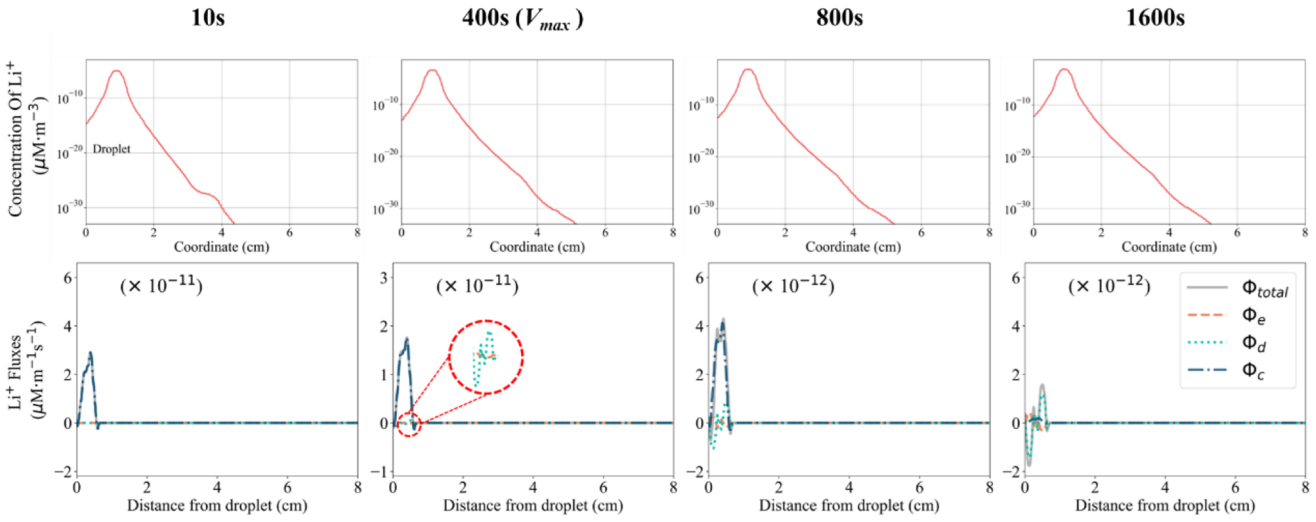

Figure 3. Temporal results for the concentration of Li^+ ions and the driving force of the ion flux during simulation. The driving force is decomposed into convective (ϕ_c), diffusive (ϕ_d), and electrophoretic (ϕ_e) flux.

the highest maximum voltage and the greatest proportion of the salt effect on voltage increase followed by NaCl and KCl, respectively.

3.2. Underlying Mechanism of Salt Ions on the Hydrovoltaic. To investigate the reason for the increasing voltage in the order of LiCl, NaCl, and KCl, we analyzed the transportation of ions on the fabric. Figure 2 displays the concentration distribution of each chemical species, with the values below the scale bars representing the maximum concentration at 10 s. Note that the color map range changed for each frame because we utilized the minimum value at each time to enhance the data visualization of the change in the concentration over time. Once the droplet of the solution was placed on the left side substrate, H_2O rapidly diffused toward the opposite dry region due to the large difference in initial concentrations. Additionally, H_3O^+ and OH^- also moved toward the dry region because of the concentration difference generated by self-dissociation and reaction with the carbon surface.[26] Furthermore, the H_3O^+ transportation rate is faster than that of OH^- on the substrate. These results are consistent not only across all solutions of LiCl, NaCl, and KCl but also with the results observed in the previous study that focused on DI water only.[26] Based on these results, it is deduced that the difference of voltage output between the solutions is a result of variations in the distribution of each salt ion's concentration and their respective streaming potential.

At the maximum voltage (t = 400 s), the concentration of salt ions on the left side of the substrate increased in the following order: Li^+, Na^+, and K^+, as shown in Figure 2. These results provide an explanation for the observed increase in voltage in the same order of LiCl, NaCl, and KCl in Figure 1a. The higher concentration of cations on the left side leads to an increased level of charge asymmetry, resulting in a strong potential difference.[29] Additionally, it was observed that the flow rate of cations was faster over time in the same order, as shown in Figure 2. When cations flow rapidly, they interact

https://doi.org/10.1021/acs.jpcc.3c03183
J. Phys. Chem. C 2023, 127, 16811−16817

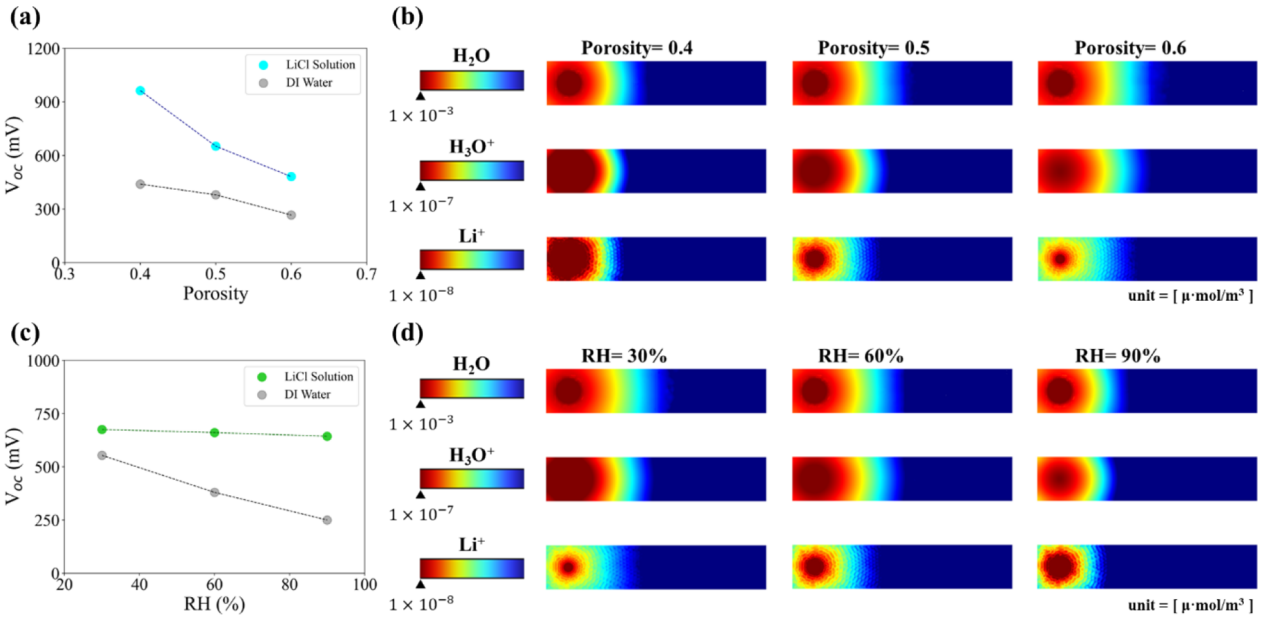

Figure 4. Open-circuit voltages and the concentration of chemical species as a function of parameters at 400 s. Note that the color range is adjusted at each parameter for easy visualization. (a) Output voltage with different porosities (ϵ_p) and (b) surface concentration gradient of H_2O, H_3O^+, and Li^+ with different ϵ_p. Note that the values below the scales are for a porosity of 0.5. (c) Output voltage with different relative humidities (RH_r) at the right side of the substrate and (d) surface concentration gradient of H_2O, H_3O^+, and Li^+ with different RH_r. Note that the values below the scales are for an RH of 60%.

with the CB surface over a wider area, leading to the formation of an EDL (electric double layer) in a larger region. The wider distribution of the EDL results in a greater asymmetry in charge distribution between the two ends of the substrate, which generates a stronger potential difference. Based on these results, it is suggested that the transportation of ions plays a key role in hydrovoltaic.

To analyze the driving force behind the movement of salt ions, the concentration and flux of Li^+ ions, which generate the highest voltage, are presented in Figure 3. The total flux (ϕ_{total}) is composed of convective (ϕ_c), diffusive (ϕ_d), and electrophoretic (ϕ_e) flux, and each component is driven by the flow of the bulk liquid, differences in concentration, and charge gradient, respectively. For $t \leq 400$ s, the rapid increase in the concentration of the Li^+ ion is dominantly influenced by convection due to the high concentration gradient of H_2O in the initial stage. After reaching the maximum voltage (t = 400 s), the rate of increase in the Li^+ concentration slows down because the dissociation of H_2O into H_3O^+ and OH^- reduces the effect of ϕ_c. Furthermore, the relatively slower driving force of ϕ_d that developed at t = 400 s gradually becomes dominant, leading to the observed results. Based on these results, we suggest that the movement of the Li^+ ion is governed by ϕ_c and ϕ_d. Additionally, although ϕ_e has less of an impact on ion transport than ϕ_c and ϕ_d, it is also a crucial factor for enduring voltage generation in the salt solution. The voltage profile drops gradually after reaching its maximum voltage (Figure 1a), even though the Li^+ ion gradient is rapidly decreased by ϕ_c and ϕ_d. This is mainly due to the fact that the presence of immobilized $(C{=}O)^-$ on the CB surface impedes the movement of Li^+ ions through electrophoresis, enabling continuous voltage generation.

3.3. Various Factors Affecting the Performance. There are many factors that affect hydrovoltaic electricity generation because it is highly related to water. These factors include not only the material and geometry[26] but also environmental conditions such as relative humidity,[30] temperature,[10] evaporation rate,[3] and wind speed.[31] The principle of multiple factors and their order of sensitivity have already been investigated in the DI water condition. However, as analyzed above, there is an additional mechanism caused by the presence of salt ions in hydrovoltaic. Therefore, it is also necessary to investigate the effects of multiple factors in the electrolyte environment as well. Herein, we investigated the effect of several factors in the electrolyte environment on the performance, specifically focusing on the porosity (ϵ_p)[32] and the relative humidity (RH), which are highly related to the evaporation rate.

Figure 4a shows the open-circuit voltage (V_{OC}) at t = 400 s, which generates the maximum voltage in the standard model (ϵ_p = 0.5), as a function of porosity. The tendency that a lower ϵ_p leads to a higher voltage in LiCl solution is consistent with DI water. However, the rate of voltage increase was found to be much higher in a salt solution compared to DI water, with a 20% decrease in ϵ_p resulting in a ~40 and ~20% increase in V_{max} for a salt solution and DI water, respectively. In particular, at ϵ_p = 0.4, the hydrovoltaic generates a much higher voltage in a salt solution. These results are associated with the flow rate of water and the dissociation time of chemical species. In Figure 4b, the concentration gradients of H_2O, H_3O^+, and Li^+ were evaluated for different porosities at t = 400 s. A higher porosity leads to a fast flow of H_2O because the higher ϵ_p stimulates more evaporation on the substrate and provides abundant channels for water and ions to transport. This led to a rapid decrease in the concentration imbalance of H_3O^+ and Li^+, which is the dominant mechanism of electricity generation in hydrovoltaic. Additionally, the distribution of ions' concentration on the surface showed that the net concentration of H_3O^+ and Li^+ is higher for lower ϵ_p. This indicates that a lower ϵ_p provides enough time for the reaction (e.g., dissociation) to occur due to the slow evaporation rate and poorer channel conditions. For these reasons, a lower ϵ_p can enhance the

https://doi.org/10.1021/acs.jpcc.3c03183
J. Phys. Chem. C 2023, 127, 16811−16817

voltage generation by developing a higher concentration gradient of ions.

In addition to porosity, relative humidity (RH) is an important factor affecting electrical performance, as demonstrated in previous studies. To investigate the effect of the ion presence on voltage generation under different humidity levels, we measured the V_{OC} by changing the model such that the RH for the right side of the substrate (RH_r) was varied while the left side RH (RH_l) was fixed at 60%, as indicated in the results in Figure 4c. Interestingly, we found that electricity generation in LiCl solution is insensitive to RH, in contrast to DI water. At lower RH_r, the evaporation is more stimulated, resulting in an increasing gradient of the water concentration and promoting a rapid flow of water, as shown in Figure 4d. This leads to an increase in the proton concentration in a large area through the reaction with the CB surface, which is the dominant principle of proton generation. However, at the same time, the concentration of Li^+ ions is lower than in the case of high RH_r. This is because the fast flow of water does not allow enough time for the reaction to generate Li^+ ions. On the other hand, at high RH_r, the concentrations of H_3O^+ and Li^+ exhibit an opposite trend. This is because the reaction occurs on a smaller scale for H_3O^+, and sufficient time is available for the reaction to occur for Li^+. Based on these results, we suggest that the opposite concentration trends of H_3O^+ and Li^+ could explain why the voltage output is not sensitive to RH in aqueous solution.

4. CONCLUSIONS

In summary, we have utilized a simulation model to theoretically investigate how the presence of salt ions can affect the electrical performance of droplet-based hydrovoltaic systems. The electrical output of various salt solutions with a concentration of 0.1 M was up to twice as high as that of DI water, and we found that the concentration asymmetry of salt ions is critical in determining the electricity generation as well as protons. Moreover, we also discovered that the transport of salt ions, which is the main cause of the concentration gradient, is initially governed by the capillary force-driven water flow and gradually becomes driven by the concentration distribution, in contrast to the behavior of protons, which is controlled by diffusion and electrophoresis. In addition, we observed the effects of porosity and relative humidity on the electrical performance, which are related to the transport of ions. Interestingly, the presence of salt ions leads to higher voltage generation as porosity decreases while made less sensitive to humidity. Our findings identify the role of salt ions in droplet-based electricity generation and can pave the way for practical hydrovoltaic systems by developing our droplet-based model to other models (e.g., immersed and moisture).

■ ASSOCIATED CONTENT

Supporting Information

The Supporting Information is available free of charge at https://pubs.acs.org/doi/10.1021/acs.jpcc.3c03183.

Photograph and XPS results of carbon black-coated cotton fabric (PDF)

■ AUTHOR INFORMATION

Corresponding Authors

Seokhee Lee − *Carbon Neutrality and Digitalization Division, Korea Institute of Ceramic Engineering and Technology (KICET), Jinju, Gyeongsangnam-do 52851, Republic of Korea*; Email: lsh@kicet.re.kr

Sung Beom Cho − *Department of Materials Science and Engineering, Ajou University, Suwon, Gyeonggi-do 16499, Republic of Korea; Department of Energy Systems Research, Ajou University, Suwon 16499, Republic of Korea*; orcid.org/0000-0002-3151-0113; Email: csb@ajou.ac.kr

Authors

Min Sung Kang − *Department of Materials Science and Engineering, Ajou University, Suwon, Gyeonggi-do 16499, Republic of Korea; Department of Energy Systems Research, Ajou University, Suwon 16499, Republic of Korea*

Hyunseok Ko − *Center of Materials Digitalization, Korea Institute of Ceramic Engineering and Technology (KICET), Jinju, Gyeongsangnam-do 52851, Republic of Korea*; orcid.org/0000-0002-1891-6194

Complete contact information is available at: https://pubs.acs.org/10.1021/acs.jpcc.3c03183

Notes

The authors declare no competing financial interest.

■ ACKNOWLEDGMENTS

This research was supported by the National R&D Program through the National Research Foundation of Korea (NRF) funded by the Ministry of Science and ICT (RS-2023-00209910).

■ REFERENCES

(1) Zhang, Z.; Li, X.; Yin, J.; Xu, Y.; Fei, W.; Xue, M.; Wang, Q.; Zhou, J.; Guo, W. Emerging Hydrovoltaic Technology. *Nat. Nanotechnol.* **2018**, *13*, 1109−1119.

(2) Yin, J.; Zhou, J.; Fang, S.; Guo, W. Hydrovoltaic Energy on the Way. *Joule* **2020**, *4*, 1852−1855.

(3) Xue, G.; Xu, Y.; Ding, T.; Li, J.; Yin, J.; Fei, W.; Cao, Y.; Yu, J.; Yuan, L.; Gong, L.; et al. Water-Evaporation-Induced Electricity with Nanostructured Carbon Materials. *Nat. Nanotechnol.* **2017**, *12*, 317−321.

(4) Yun, T. G.; Bae, J.; Rothschild, A.; Kim, I.-D. Transpiration Driven Electrokinetic Power Generator. *ACS Nano* **2019**, *13*, 12703−12709.

(5) Cheng, H.; Huang, Y.; Zhao, F.; Yang, C.; Zhang, P.; Jiang, L.; Shi, G.; Qu, L. Spontaneous Power Source in Ambient Air of a Well-Directionally Reduced Graphene Oxide Bulk. *Energy Environ. Sci.* **2018**, *11*, 2839−2845.

(6) Huang, Y.; Cheng, H.; Yang, C.; Yao, H.; Li, C.; Qu, L. All-Region-Applicable, Continuous Power Supply of Graphene Oxide Composite. *Energy Environ. Sci.* **2019**, *12*, 1848−1856.

(7) Shen, D.; Xiao, M.; Zou, G.; Liu, L.; Duley, W. W.; Zhou, Y. N. Self-Powered Wearable Electronics Based on Moisture Enabled Electricity Generation. *Adv. Mater.* **2018**, *30*, No. e1705925.

(8) Liu, X.; Gao, H.; Ward, J. E.; Liu, X.; Yin, B.; Fu, T.; Chen, J.; Lovley, D. R.; Yao, J. Power Generation from Ambient Humidity Using Protein Nanowires. *Nature* **2020**, *578*, 550−554.

(9) Qin, Y.; Wang, Y.; Sun, X.; Li, Y.; Xu, H.; Tan, Y.; Li, Y.; Song, T.; Sun, B. Constant Electricity Generation in Nanostructured Silicon by Evaporation-Driven Water Flow. *Am. Ethnol.* **2020**, *132*, 10706−10712.

(10) Shao, B.; Song, Z.; Chen, X.; Wu, Y.; Li, Y.; Song, C.; Yang, F.; Song, T.; Wang, Y.; Lee, S.-T.; et al. Bioinspired Hierarchical Nanofabric Electrode for Silicon Hydrovoltaic Device with Record Power Output. *ACS Nano* **2021**, *15*, 7472−7481.

(11) Xu, T.; Ding, X.; Huang, Y.; Shao, C.; Song, L.; Gao, X.; Zhang, Z.; Qu, L. An Efficient Polymer Moist-Electric Generator. *Energy Environ. Sci.* **2019**, *12*, 972−978.

(12) Liu, C.; Wang, S.; Wang, X.; Mao, J.; Chen, Y.; Fang, N. X.; Feng, S.-P. Hydrovoltaic Energy Harvesting from Moisture Flow Using an Ionic Polymer−Hydrogel−Carbon Composite. *Energy Environ. Sci.* **2022**, *15*, 2489−2498.
(13) Mandal, S.; Roy, S.; Mandal, A.; Ghoshal, T.; Das, G.; Singh, A.; Goswami, D. K. Protein-Based Flexible Moisture-Induced Energy-Harvesting Devices As Self-Biased Electronic Sensors. *ACS Appl. Electron. Mater.* **2020**, *2*, 780−789.
(14) Shen, D.; Xiao, M.; Xiao, Y.; Zou, G.; Hu, L.; Zhao, B.; Liu, L.; Duley, W. W.; Zhou, Y. N. Self-Powered, Rapid-Response, and Highly Flexible Humidity Sensors Based on Moisture-Dependent Voltage Generation. *ACS Appl. Mater. Interfaces* **2019**, *11*, 14249−14255.
(15) Li, X.; Ning, X.; Li, L.; Wang, X.; Li, B.; Li, J.; Yin, J.; Guo, W. Performance and Power Management of Droplets-Based Electricity Generators. *Nano Energy* **2022**, *92*, No. 106705.
(16) Zhou, G.; Ren, Z.; Wang, L.; Wu, J.; Sun, B.; Zhou, A.; Zhang, G.; Zheng, S.; Duan, S.; Song, Q. Resistive Switching Memory Integrated with Amorphous Carbon-Based Nanogenerators for Self-Powered Device. *Nano Energy* **2019**, *63*, No. 103793.
(17) He, H.; Zhao, T.; Guan, H.; Zhong, T.; Zeng, H.; Xing, L.; Zhang, Y.; Xue, X. A Water-Evaporation-Induced Self-Charging Hybrid Power Unit for Application in the Internet of Things. *Sci. Bull.* **2019**, *64*, 1409−1417.
(18) Wang, X.; Lin, F.; Wang, X.; Fang, S.; Tan, J.; Chu, W.; Rong, R.; Yin, J.; Zhang, Z.; Liu, Y.; et al. Hydrovoltaic Technology: From Mechanism to Applications. *Chem. Soc. Rev.* **2022**, *51*, 4902−4927.
(19) Shen, D.; Duley, W. W.; Peng, P.; Xiao, M.; Feng, J.; Liu, L.; Zou, G.; Zhou, Y. N. Moisture-Enabled Electricity Generation: From Physics and Materials to Self-Powered Applications. *Adv. Mater.* **2020**, *32*, 2003722.
(20) Huang, Y.; Cheng, H.; Qu, L. Emerging Materials for Water-Enabled Electricity Generation. *Acs Mater. Lett.* **2021**, *3*, 193−209.
(21) Olthuis, W.; Schippers, B.; Eijkel, J.; van den Berg, A. Energy from Streaming Current and Potential. *Sens. Actuators, B* **2005**, *111*, 385−389.
(22) Riad, A.; Khorshidi, B.; Sadrzadeh, M. Analysis of Streaming Potential Flow and Electroviscous Effect in a Shear-Driven Charged Slit Microchannel. *Sci. Rep.* **2020**, *10*, 18317.
(23) Jin, H.; Yoon, S. G.; Lee, W. H.; Cho, Y. H.; Han, J.; Park, J.; Kim, Y. S. Identification of Water-Infiltration-Induced Electrical Energy Generation by Ionovoltaic Effect in Porous CuO Nanowire Films. *Energy Environ. Sci.* **2020**, *13*, 3432−3438.
(24) Yoon, S. G.; Yang, Y.; Yoo, J.; Jin, H.; Lee, W. H.; Park, J.; Kim, Y. S. Natural Evaporation-Driven Ionovoltaic Electricity Generation. *ACS Appl. Electron. Mater.* **2019**, *1*, 1746−1751.
(25) Král, P.; Shapiro, M. Nanotube Electron Drag in Flowing Liquids. *Phys. Rev. Lett.* **2001**, *86*, 131−134.
(26) Ko, H.; Son, W.; Kang, M. S.; Lee, H. U.; Chung, C.-Y.; Han, S.; Choi, C.; Cho, S. B. Why Does Water in Porous Carbon Generate Electricity? Electrokinetic Role of Protons in a Water Droplet-Induced Hydrovoltaic System of Hydrophilic Porous Carbon. *J. Mater. Chem. A* **2023**, *11*, 1148−1158.
(27) Wu, M.; Peng, M.; Liang, Z.; Liu, Y.; Zhao, B.; Li, D.; Wang, Y.; Zhang, J.; Sun, Y.; Jiang, L. Printed Honeycomb-Structured Reduced Graphene Oxide Film for Efficient and Continuous Evaporation-Driven Electricity Generation from Salt Solution. *ACS Appl. Mater. Interfaces* **2021**, *13*, 26989−26997.
(28) Richards, L. A. CAPILLARY CONDUCTION OF LIQUIDS THROUGH POROUS MEDIUMS. *Physics* **1931**, *1*, 318−333.
(29) Zhao, F.; Liang, Y.; Cheng, H.; Jiang, L.; Qu, L. Highly Efficient Moisture-Enabled Electricity Generation from Graphene Oxide Frameworks. *Energy Environ. Sci.* **2016**, *9*, 912−916.
(30) Ren, G.; Hu, Q.; Ye, J.; Liu, X.; Zhou, S.; He, Z. Hydrovoltaic Effect of Microbial Films Enables Highly Efficient and Sustainable Electricity Generation from Ambient Humidity. *Chem. Eng. J.* **2022**, *441*, No. 135921.
(31) Ding, T.; Liu, K.; Li, J.; Xue, G.; Chen, Q.; Huang, L.; Hu, B.; Zhou, J. All-Printed Porous Carbon Film for Electricity Generation from Evaporation-Driven Water Flow. *Adv. Funct. Mater.* **2017**, *27*, 1700551.
(32) Park, J. H.; Park, S. H.; Lee, J.; Lee, S. J. Solar Evaporation-Based Energy Harvesting Using a Leaf-Inspired Energy-Harvesting Foam. *ACS Sustainable Chem. Eng.* **2021**, *9*, 5027−5037.

https://doi.org/10.1021/acs.jpcc.3c03183
J. Phys. Chem. C 2023, 127, 16811−16817